Journal of Power Sources 196 (2011) 709–716

Contents lists available at ScienceDirect

Journal of Power Sources

journal homepage: www.elsevier.com/locate/jpowsour

Effect of weave tightness and structure on the in-plane and through-plane air permeability of woven carbon fibers for gas diffusion layers

Terry B. Caston, Andrew R. Murphy, Tequila A.L. Harris*

Department of Mechanical Engineering, Georgia Institute of Technology, Atlanta, GA, United States

ARTICLE INFO

Article history:
Received 7 June 2010
Received in revised form 15 July 2010
Accepted 20 July 2010
Available online 30 July 2010

Keywords:
Gas diffusion layer
Permeability
Porosity
Tightness
Fuel cell
Woven

ABSTRACT

In this study, woven gas diffusion layers (GDLs) with varying weave type and tightness are investigated. Plain and twill weave patterns were manufactured in-house. The in-plane and through-plane air permeability of the woven samples were tested, and mercury intrusion porosimetry (MIP) tests were performed to study the pore structure. It was found that the twill weave has a higher permeability than the plain weave, which is consistent with literature. Like non-woven carbon papers, woven GDLs have higher in-plane permeability than through-plane permeability; however it has been shown that it is possible to manufacture a GDL with higher through-plane permeability than in-plane permeability. It was also concluded that the percentage of macropores in the weave is the driving factor in determining the through-plane air permeability. This work lays the groundwork for future studies to attempt to characterize the relationship between the weave structure and the air permeability in woven GDLs.

1. Introduction

The maturing field of polymer electrolyte membrane (PEM) fuel cells has shown promise as a non-polluting, energy efficient power source for portable devices, stationary applications and the transportation sector. The gas diffusion layer (GDL) is a major component of the membrane electrode assembly of the fuel cell. The GDL is either made of carbon paper, which is manufactured by pressing carbon fibers into a paper, or by weaving carbon cloth [1]. GDLs perform essential functions in PEM fuel cells including: (1) conducting electrons from the catalyst sites to the bipolar plate, (2) removing heat and water produced in the electrochemical reactions, (3) providing a mechanical backing for the membrane electrode assembly, and (4) assisting in distributing the reactants evenly over the face of the electrode.

GDLs have a porous structure which allows for the transport of reactant gases from the bipolar plate to the catalyst; and on the cathode side the porous structure assists in the removal of water produced in the electrochemical reaction. At higher current densities, water can block the pores in the GDL and inhibit the reactant gases from reaching the active sites in the catalyst layer [2,3]. In regions starved for reactants generated heat can lead to mechanical failure; while, a lack of water in the membrane can lead to a significant drop in performance [3,4].

It is well understood that the Darcy–Forchheimer equation, given by Eq. (1), describes the relationship between the pressure drop and the flow velocity of a single-phase flow through a porous media [5,6].

$$-\nabla P = \frac{\mu}{K}v + \beta\rho v^2 \quad (1)$$

where P is the pressure, μ is the dynamic viscosity, K is the absolute permeability, v is the superficial velocity, β is the Forchheimer coefficient and ρ is the density of the impregnating fluid. In this model, the viscosity of the impregnating fluid depends on the fuel composition and the velocity can be controlled, however, the permeability of the porous medium is an intrinsic property based on the structure of the material [7]. To this end, it is important to understand how physical parameters affect the transport properties of the GDL in order to better control the transport and achieve optimal performance.

Much work has been conducted to characterize the transport properties of the GDL using numerical and experimental approaches. Pharoah used computational fluid dynamics (CFD) to show that convective flow in the GDL is important at permeability values higher than 1×10^{-12} m^2, and that in-plane permeability is more dominant than through-plane permeability when considering orthotropic permeability. However, it is noted that little work has been conducted to consider anisotropic permeability [8]. In a follow-up study, Pharoah et al. compared computational models considering isotropic permeability with models considering anisotropic permeability and found that the models considering only isotropic permeability over predicts performance [9].

* Corresponding author. Tel.: +1 404 385 6335; fax: +1 404 894 9342.
E-mail address: tequila.harris@me.gatech.edu (T.A.L. Harris).

0378-7753/$ – see front matter © 2010 Elsevier B.V. All rights reserved.
doi:10.1016/j.jpowsour.2010.07.057

A limitation of Pharoah et al.'s anisotropic model, which was developed by Tomadakis and Sotirchos [10,11], is that it represents the permeability of randomly oriented fibers distributed in a plane, making the model useful for carbon paper, but not woven GDLs. Consequently, this model cannot describe the anisotropic properties of woven GDLs.

In addition to numerical studies, a number of groups have conducted experimental work to measure the in-plane and through-plane gas permeability of GDLs. Feser et al. used a radial flow apparatus to measure the in-plane permeability of carbon paper, non-woven carbon fiber structure and carbon cloth under different levels of compression. They found that the non-woven carbon fiber structures had higher in-plane permeability than the carbon paper, but made no further comments to how the structure affects permeability [12]. Gurau et al. [7] tested the in-plane and through-plane permeability of four samples of carbon cloth with different microporous layers and one sample without a microporous layer to determine the permeability coefficients of the microporous layers. They found the in-plane and through-plane permeability values to be approximately $1 \times 10^{-12}\,m^2$ and $20 \times 10^{-12}\,m^2$, respectively, and that the in-plane permeability tends to be higher than the through-plane permeability. Gurau et al. determined that more polytetrafluoroethylene (PTFE) in the microporous layers increased the permeability, which is contrary to literature which suggests that a higher PTFE content blocks pores and decreases air flow [7]. Ismail et al. [6] tested the through-plane permeability of a variety of untreated and PTFE-treated GDLs using and in-house test device. They found there was an optimal amount of PTFE loading where the through-plane permeability is highest [6]. Williams et al. measured the through-plane permeability and tested the performance of four commercial carbon papers, three commercial carbon cloths and carbon paper manufactured in-house [13]. They concluded that the limiting current increases with higher permeability because the GDL can remove excess water produced at higher current density that blocks the pores. Gostick et al. characterized the in-plane permeability of five carbon papers and one woven carbon fiber structure under different levels of compression using a parallel channel flow device. Using a different device to measure the through-plane permeability, they found most materials are anisotropic. They further showed that the in-plane permeability is higher than the through-plane permeability, which is consistent with literature [5].

To the authors' knowledge, there are no previous studies which correlate the structure of woven GDLs to their permeability. There are studies in textile research which study the permeability of woven textiles, which are likely similar to woven carbon fibers. These studies are limited to focus through-plane permeability. For instance, Feather and Anderson measured the permeability of plain, twill and hopsack weaves with varying tightness by increasing the number of fibers per unit length [14]. They found that the through-plane permeability decreased as the linear density of the fiber increased. They also found that the plain weave had the lowest air permeability of all structures tested. Epps and Leonas investigated the permeability of 10 different woven fabrics with a liquid porosimetry technique. They found that the permeability is highly correlated to the minimum pore size, but also depends on the mean pore size and porosity [15]. Ogulata studied the air permeability of woven structures with a different number of weft yarns per cm. He found that the permeability decreased with an increasing number of weft fibers per cm, which shows a correlation between the porosity and the air permeability [16]. As the number of fibers increase, there is less void space between fibers, which decreases porosity and air permeability. Therefore, porosity is a measure of the amount of void space in a woven fabric, while permeability is a measure of the resistance to flow by an impregnating fluid [16]. Further, permeability is determined by the structure of the weave, the amount of twist in the tows, the size of the tows and the density of tows in the weave [15].

While some experiments have been conducted to measure the permeability of carbon paper and woven GDLs, limited work has been conducted to characterize the transport properties of woven carbon fiber materials. Emerging fuel cell concepts require higher through-plane permeability than in-plane permeability [17]; however, conventional GDLs exhibit a permeability profile with an in-plane permeability which is twice the through-plane permeability. Thus a method to control the permeability through the GDL is of interest. In this study, GDLs with varying weave type and tightness, manufactured in-house, have been considered. The through-plane and in-plane permeability of the GDLs were tested on devices built in-house, and their pore structure was analyzed based on mercury intrusion porosimetry (MIP) tests. The pore structure was correlated to the permeability, which was analyzed with respect to weave type and weave tightness, to illustrate that higher through-plane than in-plane permeability is feasible.

2. Materials and methods

2.1. Materials

To validate the accuracy of the test equipment, a non-woven carbon paper material, SGL 34BA (SGL Technologies, GmbH) was compared to results presented by Gostick et al. [5]. The carbon paper had a thickness of 285 μm, which was verified with a Mitutoyo micrometer (±10 μm). The woven GDL samples were composed of T-300 carbon fibers provided by Cytec Inc. Each T-300 carbon fiber strand contains 3000 individual carbon fibers. Samples were made in-house using a weaving loom to construct plain and twill weave patterns.

2.2. Weaving loom

Woven fabrics are manufactured by interlacing warp and weft fibers, called tows. Warp tows are along the length of the fabric, while weft tows are along the width of the fabric, as shown in Fig. 1. In a plain weave, one weft tow repeats a simple over/under pattern as seen in the plain woven fabric in Fig. 1. In a twill weave, the weft tow is passed over two warp fibers before it passes under two weft fibers. This over-two under-two pattern continuously repeats as seen in Fig. 2.

The woven plain and twill GDLs were made on a 16″ Ashford 8 harness hand loom, shown in Fig. 3. The warp fibers were fixed to the weaving loom on a ruler at the desired spacing corresponding to the desired tightness. The weft fibers were inserted between the warp fibers and pushed into the weave pattern with a beater. After two fibers were inserted, the spacing between the weft fibers was measured to ensure the desired tightness was obtained.

2.3. Through-plane permeability test set-up

The through-plane permeability test system was based on the system used by Gostick et al. [5] and is shown in Fig. 4(a) and (b). A 1.5 cm × 1.5 cm woven sample was placed between the two metal plates and bolted down. Air flow was controlled using the Alicat Scientific mass flow controller. The pressure drop was measured using a low pressure differential pressure sensor (Omega PX-653) that measures from −12.5 Pa to 12.5 Pa with an accuracy of ±0.1%. A mixture of soap and water was applied to the sides of the device to ensure a gas tight seal, which was easily obtained due to the low pressure drop. Four samples of each weave design were measured.

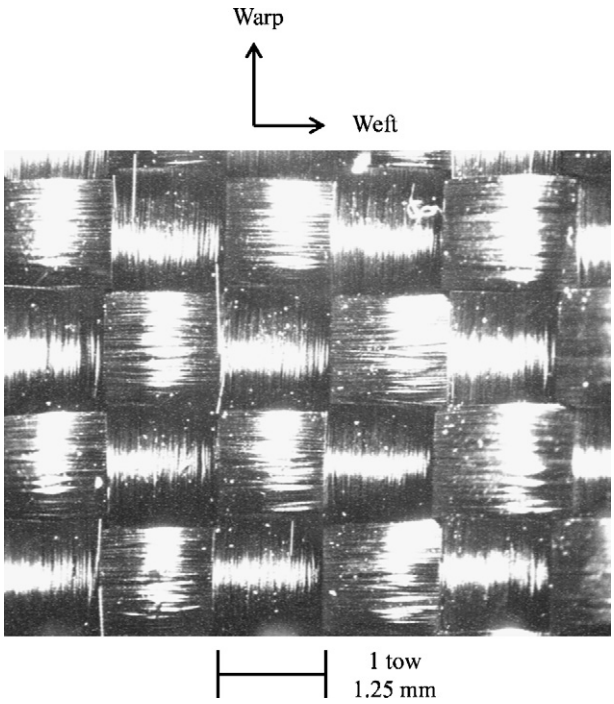

Fig. 1. Plain weave.

2.4. In-plane permeability test set-up

The in-plane permeability test system was based on the test system used by Gostick et al. [5] and is shown in Fig. 5(a) and (b). A 1.5 cm × 1.5 cm woven sample was placed between two parallel channels which were then clamped down onto feeler gauges of a known thickness. The air flow to the system was adjusted using an Alicat Scientific mass flow controller that measures 0–0.08 standard cubic centimeters per minute (SCCM) with an accuracy of ±0.4%, reading ±0.2% full scale. The pressure at the inlet was measured using the mass flow controller, and the pressure at the outlet was taken as atmospheric pressure. To prevent air leakage, a malleable plumber's putty was spread along the back of the channels, while rubber gaskets were used to seal leak points in the side panels. Before each test, the system was pressurized to 275 kPa gauge to ensure there were no external leaks. Tests were completed without a sample to verify the open channel induced a negligible pressure drop. In-plane permeability data was measured for three levels of compression, and tests were repeated.

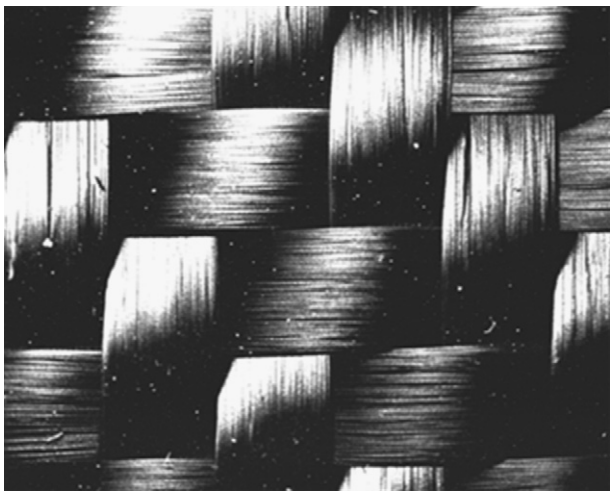

Fig. 2. Twill weave.

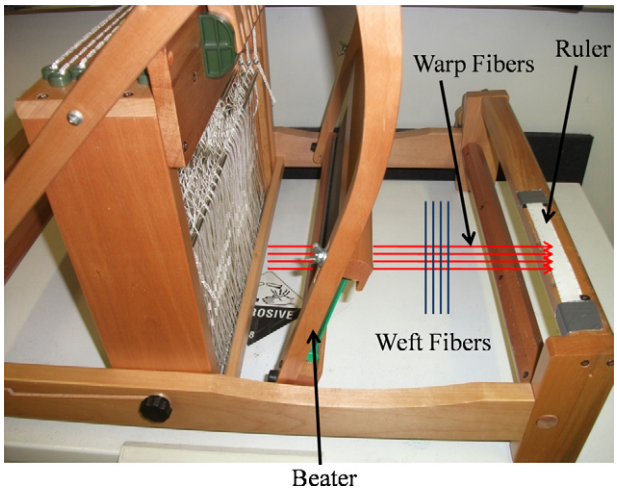

Fig. 3. Weaving Loom.

3. Data analysis

3.1. Permeability calculation

As was discussed in Section 1, the Darcy–Forchheimer equation, given by Eq. (1), relates the pressure drop to the velocity in a porous medium. Assuming 1-D compressible flow, which is reasonable given that air is compressible and that the flow is driven in one direction by the pressure source, an alternate form of the

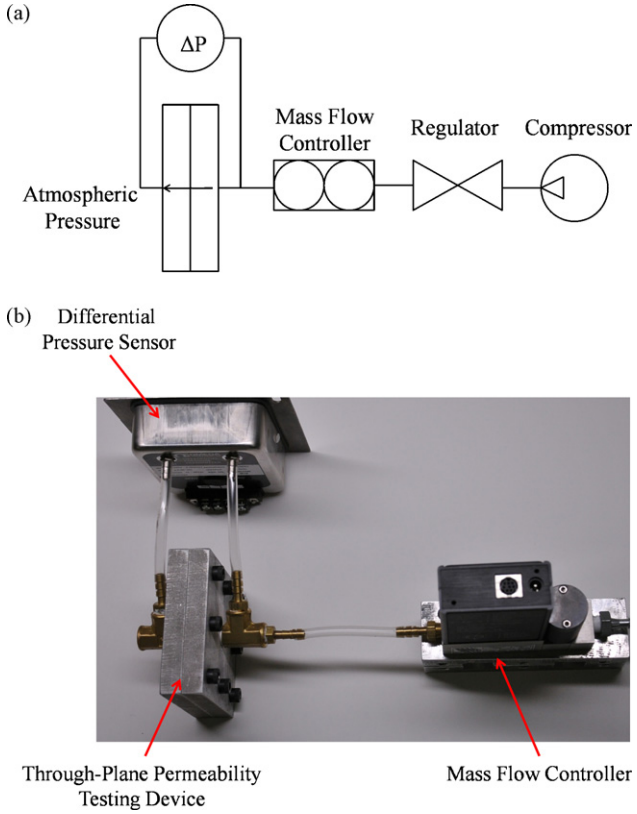

Fig. 4. (a) Through-plane permeability test set-up and (b) through-plane permeability test device.

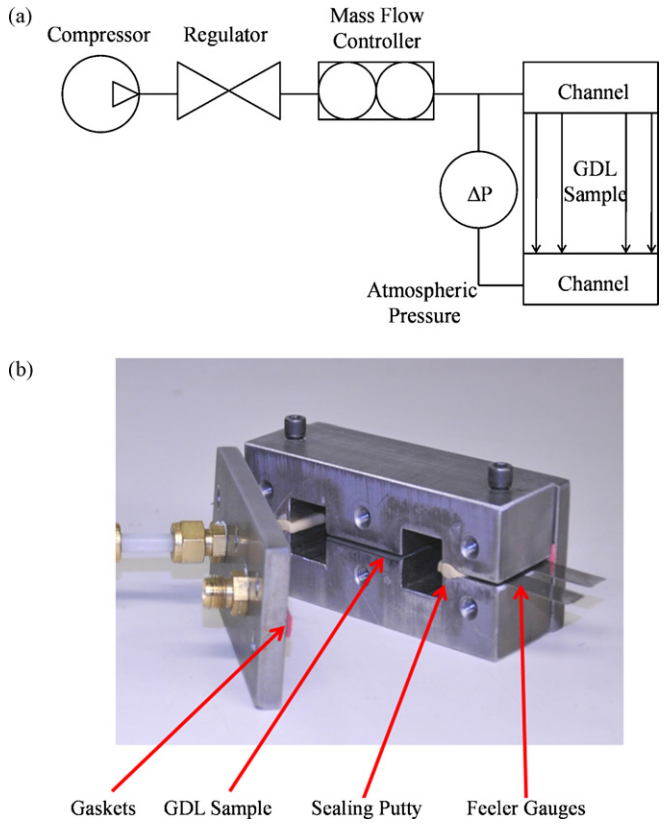

Fig. 5. (a) In-plane permeability test set-up and (b) in-plane permeability test device.

Darcy–Forchheimer equation can be derived, given by Eq. (2) [6],

$$\frac{P_{in}^2 - P_{out}^2}{2LRT} M = \frac{\mu}{K} m' + \beta m'^2 \quad (2)$$

where P_{in} is the absolute pressure at the inlet, P_{out} is the absolute pressure at the outlet, L is the distance the gas travels through the porous medium, R is the universal gas constant, T is the temperature in Kelvin, M is the molecular weight of the impregnating gas and m' is the mass flux of the gas through the porous medium. After measuring the inlet and outlet pressure for a sample at a given mass flow rate, the mass flux can be plotted against the pressure term on the left hand side of Eq. (2), as seen for a typical sample in Fig. 6. Using Microsoft Excel 2007, a 2nd order polynomial can then be fit to the data, which was compared to Eq. (2). Assuming a constant

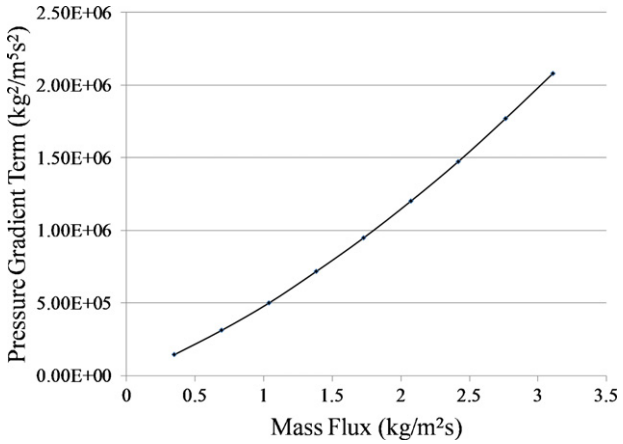

Fig. 6. Representative plot of pressure gradient vs. mass flux.

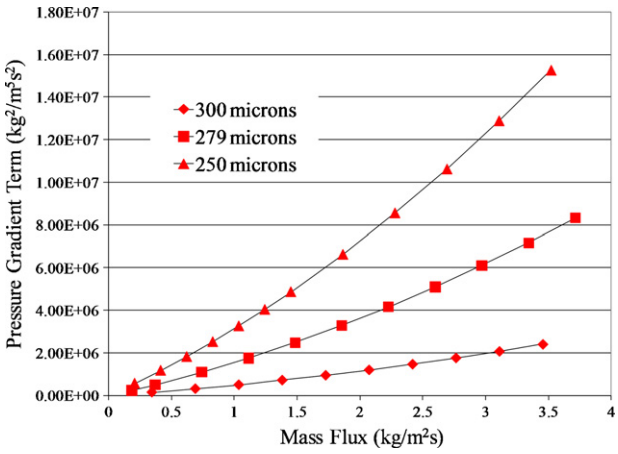

Fig. 7. Twill 8 × 4 sample under three levels of compression.

viscosity of 1.85×10^{-5} Pa s, the linear term of the polynomial can be used to calculate the permeability. This method was used to calculate the permeability in this study.

3.2. Calculation of uncompressed permeability for in-plane tests

During the in-plane permeability tests, the permeability of the samples was measured under compression; however the uncompressed permeability is desired. Thus, a relationship between the compressed porosity and the permeability was used to calculate the uncompressed in-plane permeability from the compressed permeability values measured. A sample was compressed to three known thicknesses, using feeler gauges to control the thickness, and the pressure gradient term was plotted against the mass flux for each level of compression, as seen in Fig. 7 for a twill 8 × 4 sample. Using the analysis in Section 3.1, the permeability was calculated at each level of compression.

Assuming incompressible fibers and all the reduction in volume is due to reduction of the pore size, the compressed pore porosity is given by Eq. (3) [5].

$$\varepsilon_C = \frac{V_{p,C}}{V_{b,C}} = 1 - \frac{1-\varepsilon_0}{V_{b,C}/V_{b,0}} \quad (3)$$

where ε_C is the compressed porosity of the sample, $V_{p,C}$ is the compressed pore volume, $V_{b,C}$ is the compressed volume of the bulk volume of the sample, ε_0 is the original porosity and $V_{b,0}$ is the original bulk volume of the sample. After calculating the porosity at each level of compression, the porosity can be plotted against the permeability, as shown in Fig. 8. An exponential curve can be fit to the data and the uncompressed permeability can be calculated using the curve fit and the uncompressed porosity. This method was used to calculate the in-plane permeability in this study.

4. Results and discussion

4.1. Design of experiments

The linear fiber density (i.e., number of fibers per unit length) was varied over a range for plain and twill woven structures. The carbon fiber tows used to weave the GDLs were 1.25 mm in diameter as shown previously in Fig. 1. Thus, the maximum tightness that could be woven without deforming the fibers is 8 fibers per cm. For any given sample, 8 tows were maintained in the warp direction while the number of tows in the weft direction ranged from 4 to 8. Woven structures with 8 fibers per cm in the warp and

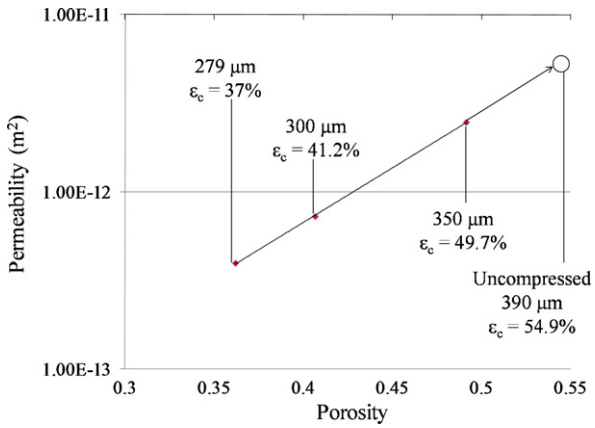

Fig. 8. Permeability vs. porosity for a twill 8 × 8 sample.

Table 1
Weave samples.

Plain weave (tows cm^{-1} warp × weft)	Twill weave (tows cm^{-1} warp × weft)
8 × 8	8 × 8
8 × 6	8 × 6
8 × 4	8 × 4

weft direction were classified as an 8 × 8 weave, which is the maximum tightness. When the number of tows in the weft direction was less than 4, the sample could not sustain its structure so an 8 × 4 weave was the loosest weave studied. The two weave types and the respective weave tightnesses are illustrated in Table 1.

4.2. Through-plane permeability results

The through-plane permeability was tested with the set-up shown in Fig. 4. Before the woven samples were tested, the carbon paper material, SGL 34 BA, was tested and compared to the results reported by Gostick. The through-plane permeability for SGL 34 BA was measured as 8.4×10^{-12} m^2, while the through-plane permeability reported by Gostick et al. for the same material was 16.1×10^{-12} m^2. Although the permeability measured is one-half the permeability reported by Gostick et al., this is still considered reasonable. For a similar material, SGL 10 BA, Ihonen et al. [18] reported a value of 18×10^{-12} m^2, while Gostick et al. reported a value of 37.4×10^{-12} m^2, which are also different by a factor of two. Furthermore, since the range of permeability values reported in literature is between 10^{-12} and 10^{-10} m^2, this factor of two seems insignificant and is considered acceptable for this study. The through-plane permeability for the samples tested is shown in Table 2.

As shown in Table 2, the through-plane permeability of the 8 × 4, 8 × 6, and 8 × 8 twill weave structures is 4.6, 14.8 and 2.7 times higher than the permeability of the 8 × 4, 8 × 6, and 8 × 8 plain weave structures, respectively. This is consistent with literature which states that the plain weave exhibits the lowest through-plane permeability. It is expected that the permeability will decrease as the weave tightness increases because there is more solid volume per unit area. This trend is seen with the twill weave, as shown in Fig. 9. The loosest weave have the highest permeability (i.e., 8 × 4) and as the weave tightness increases the permeability decreases. Conversely, this trend was not seen with the plain weave, as shown in Fig. 10. It was expected that the plain 8 × 8 would have the lowest permeability, but the plain 8 × 8 pattern had a permeability which was 2.6 times higher than the plain 8 × 6 pattern. Tests were repeated on multiple batches of samples which resulted in the same trends, thus, excluding manufacturing error as the reason for the discrepancy.

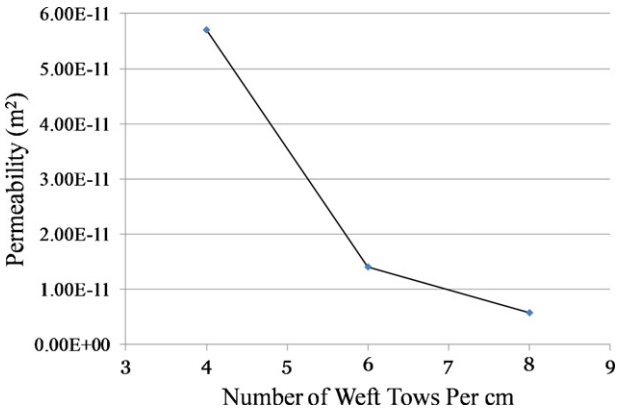

Fig. 9. Through-plane permeability of twill woven samples with varying tightness.

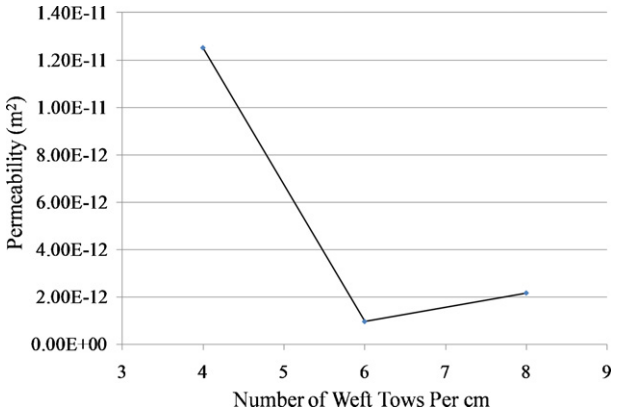

Fig. 10. Through-plane permeability of plain woven samples with varying tightness.

4.3. Mercury intrusion porosimetry

One sample of each weave pattern was sent to Micromeritics Corp., USA, for mercury intrusion porosimetry (MIP) tests to study the pore structure. The pore size distribution for the plain 8 × 8 weave is shown in Fig. 11. There are four distinct regions which correspond to four different pore sizes, including macropores, mesopores, micropores, and nanopores. The macropores (50–400 µm) represent the pores between fiber tows. The mesopores represent the pores between two interlacing fiber tows that are laid on top of one another. The micropores represent the pores

Table 2
Through-plane permeability of woven samples.

Linear density	Plain weave		Twill weave	
	Permeability × 10^{-12} (m^2)	Average deviation × 10^{-12} (m^2)	Permeability × 10^{-12} (m^2)	Average deviation × 10^{-12} (m^2)
8 × 4	12.5	±0.65	57	±3.44
8 × 6	0.95	±0.10	14.1	±1.4
8 × 8	2.15	±0.63	5.8	±0.035

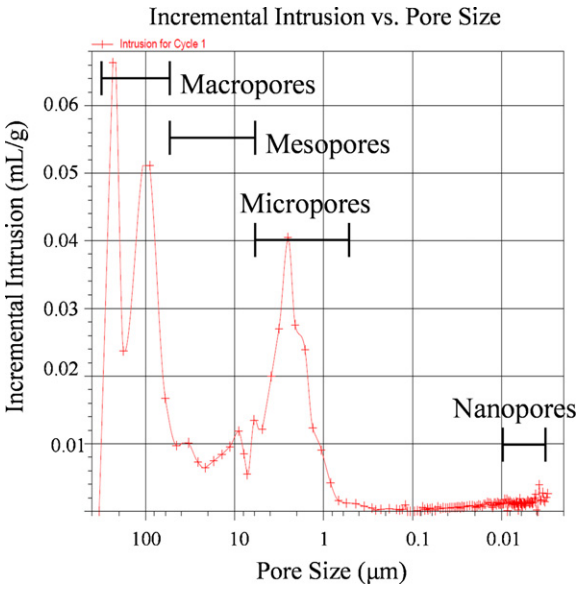

Fig. 11. Incremental intrusion vs. pore size for plain 8 × 8 weave.

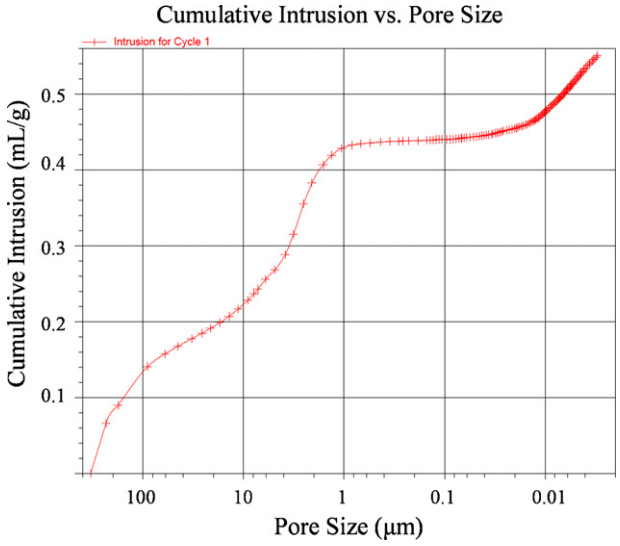

Fig. 12. Cumulative intrusion vs. pore size for a plain 8 × 8.

between individual carbon fibers in a single fiber tow, and the nanopores represent the pores within a single fiber.

To analyze the percentage of each pore type, the cumulative pore intrusion vs. the pore size was used, as shown in Fig. 12. The percentage of each pore type is shown in Table 3. The percentage of macropores for the twill weave is 42.86%, 36.84% and 30.3% for the 8 × 4, 8 × 6 and 8 × 8 samples, respectively, which is consistent with the decrease in permeability seen in tighter weaves. The percentage of macropores for the plain weave is 31.43%, 25.00% and 29.09% for

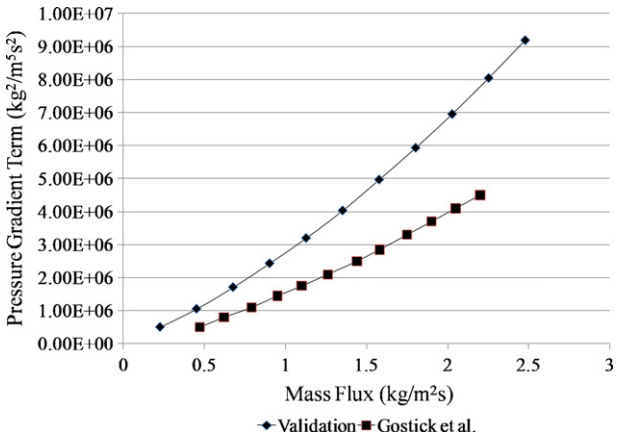

Fig. 13. In-plane permeability of SGL 34BA at a compression of 230 μm.

the 8 × 4, 8 × 6 and 8 × 8 samples, respectively, which is consistent with the shape of the through-plane permeability for plain woven structures shown in Fig. 9. The number of macropores in an 8 × 8 plain weave structure is higher than the number of macropores in an 8 × 6 plain weave structure which explains the decrease in permeability in the 8 × 6 sample. Therefore, it can be concluded that the percentage of macropores is the driving factor in determining the through-plane permeability of a woven GDL, because the macropores are larger than the other pores which results in higher permeability.

4.4. In-plane permeability results

During through-plane testing, the permeability was independent of the weave's placement in the testing device because the flow was perpendicular to the weave pattern. However, during in-plane testing, the flow entered the side of the sample and was parallel to the weave pattern. Thus, the samples were tested in both in-plane directions to investigate the anisotropic in-plane permeability. To validate the in-plane testing device and set-up, the mass flux was plotted against the pressure gradient term for SGL 34 BA at a compression of 230 μm and compared to the results reported by Gostick et al. As shown in Fig. 13, the in-plane permeability test device built in-house predicted a pressure gradient twice as high as Gostick et al. for a given mass flux. This matches the trend from the through-plane tests and is considered insignificant for this study.

The in-plane permeability was measured under three levels of compression ranging from 250 μm to 400 μm. Samples with a different linear fiber density in the warp and weft (i.e., 8 × 6 and 8 × 4) were measured in each direction. To distinguish which direction is measured, the direction reported is the number of tows cm^{-1} perpendicular to the flow (e.g., in the 8 × 4 sample, the 4 direction is the in-plane direction where the impregnating air will encounter 4 tows cm^{-1} perpendicular to the direction of flow), as illustrated in Fig. 14.

The results of the in-plane tests are shown in Table 4. The first conclusion that can be drawn from Table 4 is that in an anisotropic

Table 3
Percentage of each pore type based on mercury intrusion porosimetry.

Weave type	Macro 50–400 (μm)	Meso 5–50 (μm)	Micro 0.5–5 (μm)	Nano 0.005–0.03 (μm)
Plain 8 × 8	29.09%	12.73%	36.36%	21.82%
Plain 8 × 6	25.00%	17.86%	35.71%	21.43%
Plain 8 × 4	31.43%	34.28%	20.00%	14.29%
Twill 8 × 8	30.30%	30.31%	27.27%	12.12%
Twill 8 × 6	36.84%	26.32%	23.68%	13.16%
Twill 8 × 4	42.86%	21.42%	21.43%	14.29%

Table 4
Uncompressed in-plane permeability for woven samples.

	8 Direction (permeability $\times 10^{-12}$ m^2)	6 Direction (permeability $\times 10^{-12}$ m^2)	4 Direction (permeability $\times 10^{-12}$ m^2)
Twill 8 × 8	61.6	X	X
Twill 8 × 6	117	109	X
Twill 8 × 4	114	X	47.4
Plain 8 × 8	126	X	X
Plain 8 × 6	248	116	X
Plain 8 × 4	4860	X	321

sample the permeability is higher in the direction where the air flows perpendicular to more tows cm^{-1}. For example, the permeability for the plain 8 × 4 is 15 times higher in the 8 direction than the 4 direction. This means there is more resistance when the air flows through the length of the fiber than when the air flows perpendicular to the fiber. It would be reasonable to assume the permeability is lower in tighter woven samples (i.e., the permeability should be higher in an 8 × 4 than an 8 × 8 structure). In a tighter woven sample, the air must flow through more solid fiber per unit length which should create more resistance and a higher-pressure drop. This pattern is seen with the plain weave, where the permeability for the plain 8 × 4 is 20 and 39 times higher than plain 8 × 6 and 8 × 4, respectively. This pattern is not seen in the twill weave. The permeability for the twill 8 × 4 in the 8 direction has a 2.5% variation with the permeability for the twill 8 × 6. The permeability is also higher in the twill 8 × 6 than the twill 8 × 4 in the 8 direction. The inconsistency can possibly be explained by the difficulty in testing samples in the in-plane direction. If the sample is not the exact dimension of the sample platform (1.5 cm × 1.5 cm) air can flow around the sample rather than through the sample. When the system is pressurized and tested for external leaks it will appear leak free. However, this internal leak between the parallel channels can cause an artificial lower pressure drop which will correspond to an artificial higher permeability. Steps were taken to prevent this by cutting the samples to size once they were clamped in the device, but it is possible the samples could have moved within the device. Another possible cause of the inconsistency could be due to the destructive nature of the tests. When the sample is removed from the device and re-clamped for a new test, the compression could damage the sample and affect the results.

Comparing Tables 3 and 4, it can be seen that the in-plane permeability is higher than the through-plane permeability for the woven structures, which is consistent with the results reported in literature for non-woven structures. There is one exception, the twill 8 × 4 in the 4 direction which exhibits a through-plane permeability that is 20% higher than the in-plane permeability. This shows that it is possible to create a woven structure with higher through-plane permeability than in-plane permeability.

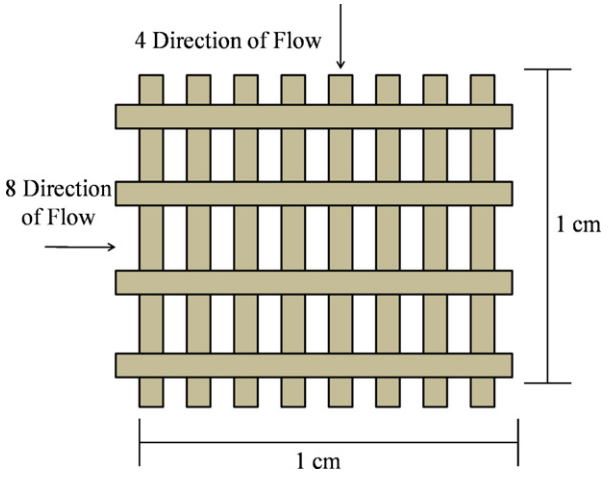

Fig. 14. Naming convention for in-plane tests.

5. Conclusions

In this study, woven GDLs with varying weave pattern and weave tightness were manufactured in-house on a handloom. The in-plane and through-plane permeability of the samples were tested and the pore structure was analyzed with mercury intrusion porosimetry in an attempt to correlate the structure to the permeability profile. It was found that the percentage of macropores is the driving factor in determining the through-plane permeability of a woven GDL. The in-plane permeability is higher than the through-plane permeability for woven GDLs, which is consistent with the permeability profile of non-woven commercial GDLs, with one exception, the twill 8 × 4 in the 4 direction, which exhibits higher through-plane permeability. This shows it is possible to manufacture GDLs with higher through-plane permeability than in-plane permeability with woven carbon fibers. While the permeability of commercial GDLs has been tested, this is the first work to attempt to relate the manufacturing and the structure to the permeability. The relevancy of this work is that there exist a trade-off between the permeability and the conductivity of GDLs. Higher porosity leads to higher permeability and lower conductivity due to the high contact resistance from the pore/carbon fiber interface. Thus having an understanding of the tightness and structure of the GDL with respect to in-plane and through-plane permeability, especially woven GDLs, is imperative.

Acknowledgements

The authors would like to acknowledge the NSF-CMMI-0928093 for partial support of this work; Cytec Inc. for providing the material used to weave the GDLs used in this study; Dr. Michael Ellis from the Virginia Polytechnic Institute for the use of his lab in evaluating the potential for the manufacturing process; and Dr. Jeff Gostick for his insight into the test set-up and trouble shooting.

References

[1] Y. Wang, C.-Y. Wang, K.S. Chen, Elucidating differences between carbon paper and carbon cloth in polymer electrolyte fuel cells, Electrochimica Acta 52 (12) (2007) 3965–3975.
[2] G. Karimi, F. Jafarpour, X. Li, Characterization of flooding and two-phase flow in polymer electrolyte membrane fuel cell stacks, Journal of Power Sources 187 (1) (2009) 156–164.
[3] D. Gerteisen, T. Heilmann, C. Ziegler, Modeling the phenomena of dehydration and flooding of a polymer electrolyte membrane fuel cell, Journal of Power Sources 187 (1) (2009) 165–181.
[4] D. Natarajan, T.V. Nguyen, Current distribution in PEM fuel cells. Part 1. Oxygen and fuel flow rate effects, AlChE 51 (9) (2005) 2587–2598.
[5] J.T. Gostick, et al., In-plane and through-plane gas permeability of carbon fiber electrode backing layers, Journal of Power Sources 162 (1) (2006) 228–238.
[6] M. Ismail, et al., Through-plane permeability for untreated and PTFE-treated gas diffusion layers in proton exchange membrane fuel cells, in: Seventh International Fuel Cell Science, Engineering and Technology Conference, Newport Beach, CA, 2009.

[7] V. Gurau, et al., Characterization of transport properties in gas diffusion layers for proton exchange membrane fuel cells: 2. Absolute permeability, Journal of Power Sources 165 (2) (2007) 793–802.
[8] J.G. Pharoah, On the permeability of gas diffusion media used in PEM fuel cells, Journal of Power Sources 144 (1) (2005) 77–82.
[9] J.G. Pharoah, K. Karan, W. Sun, On effective transport coefficients in PEM fuel cell electrodes: anisotropy of the porous transport layers, Journal of Power Sources 161 (1) (2006) 214–224.
[10] M.M. Tomadakis, S.V. Sotirchos, Effective Kundsen diffusivities in structures of randomly overlapping fibers, AIChE Journal 37 (1) (1991) 74–86.
[11] M.M. Tomadakis, S.V. Sotirchos, Ordinary and transition regime diffusion in random fiber structures, AIChE Journal 39 (3) (1993) 397–412.
[12] J.P. Feser, A.K. Prasad, S.G. Advani, Experimental characterization of in-plane permeability of gas diffusion layers, Journal of Power Sources 162 (2) (2006) 1226–1231.
[13] M.V. Williams, et al., Characterization of gas diffusion layers for PEMFC, Journal of the Electrochemical Society 151 (8) (2004) A1173–A1180.
[14] D.G. Feather, S.L. Anderson, Some physical properties of a rangeof worsted fabrics, Journal of the Textile Institute 58 (6) (1967).
[15] H.H. Epps, K.K. Leonas, The relationship between porosity and air permeability of woven textile fabrics, Journal of Testing and Evaluation 25 (1) (1997).
[16] R.T. Ogulata, Air Permeability of Woven Fabrics, Journal of Textile and Apparel, Technology and Managemenet 5 (2) (2006).
[17] K. Bhamidipati, H. Amani, S. Strauss, T.A.L. Harris, Numerical simulation of an innovative PEM fuel cell stack, in: ASME Fuel Cell Science and Technology Conference, June 2008, Paper # FuelCell2008-65167.
[18] J. Ihonen, M. Mikkola, G. Lindbergh, Flooding of gas diffusion backing in PEFCs: physical and electrochemical characterization, Journal of the Electrochemical Society 151 (8) (2004) A1152–A1161.